

Investigating radial-flow-like effects via pseudorapidity and transverse sphericity dependence of particle production in pp collisions at the LHC

Aswathy Menon K R¹, Suraj Prasad¹, Sushanta Tripathy², Neelkamal Mallick¹, and Raghunath Sahoo^{1*}

¹*Department of Physics, Indian Institute of Technology Indore, Simrol, Indore 453552, India and*

²*CERN, CH 1211, Geneva 23, Switzerland*

(Dated: September 18, 2023)

Recent observations of quark-gluon plasma (QGP) like signatures in high multiplicity proton-proton (pp) collisions, have compelled the heavy-ion physics community to re-examine the pp collisions for proper baseline studies. Event-shape-based studies in pp collisions have succeeded to a certain extent in identifying rare events mimicking such heavy-ion-like behaviour. In this manuscript, we incorporate PYTHIA8 to study radial flow-like signatures in pp collisions at $\sqrt{s} = 13$ TeV as a function of transverse sphericity and pseudo-rapidity. The pseudo-rapidity dependence would help understand the scientific community for future upgrades. At the same time, the transverse sphericity will serve its purpose of identifying soft-QCD-dominated events in small collision systems. We present the mean transverse momentum, particle ratios, and kinetic freezeout parameters as a function of transverse sphericity and pseudo-rapidity in pp collisions at $\sqrt{s} = 13$ TeV using PYTHIA8. We observe that the isotropic events show enhanced radial-flow effects and jetty events show the absence of radial-flow-like effects. For the first time, we show the transverse sphericity and pseudorapidity dependence of partonic modification factor in pp collisions, which clearly shows that by choosing transverse sphericity one can directly probe the radial-flow-like effects in pp collisions at the LHC.

I. INTRODUCTION

The primary goal of heavy-ion collisions at ultra-relativistic energies is to probe the quantum chromodynamic (QCD) phase diagram. Such collisions at the Large Hadron Collider (LHC) and Relativistic Heavy-ion collider (RHIC) form a state of deconfined partons in thermal equilibrium called the quark-gluon plasma (QGP), which is believed to have existed a few microseconds after the Bigbang. It is nearly impossible to directly observe such a deconfined medium in heavy-ion collisions at the colliders due to its short lifetime. However, there are a few indirect signatures that can signify the presence of such a medium. A few of these signatures require a baseline. Traditionally, proton-proton (pp) collisions have been used as the baseline to study these signatures for last few decades; however, recent observations of ridge-like structures [1, 2], observation of strangeness enhancement [3] and radial flow-like signatures [4–6], in high multiplicity pp collisions have impelled the scientific community to examine the origin of such observations in pp collisions.

Perturbative quantum chromodynamics (pQCD) inspired models such as PYTHIA [7] with the implementation of color reconnection (CR) and multi-partonic interactions (MPI) are able to imitate the radial flow-like effects in pp collisions [8]. The radial flow is believed to give a boost to the particles based on their transverse momentum, where higher momentum particles get a greater boost compared to the lower momentum particles for a given particle species. This transverse momentum-

dependent boost due to radial flow gives rise to the broadening of the transverse momentum spectra of the particle, thus enhancing mean transverse momenta, and it depends upon the particle mass as particles with lower mass are less affected due to this radial flow compared to the particles with higher mass [9]. This broadening of transverse momentum spectra for particles of different masses leads to a peak-like structure around 2-3 GeV/c in transverse momentum in the ratios of particle yields for different masses. In Pb–Pb collisions, the central collisions are observed to have more such radial flow effect compared to the peripheral collisions [10]. The mean transverse radial flow velocity ($\langle\beta_T\rangle$) is commonly extracted from the simultaneous Boltzmann Gibbs blastwave function fit of the identified particles' transverse momentum spectra. A study of the mean radial expansion velocity in Cu + Cu collisions at $\sqrt{s_{NN}} = 200$ GeV, when performed as a function of pseudo-rapidity, it has been observed that as one goes towards the higher rapidity, the expansion velocity reduces as the system gets less dense [11]. This mean value of radial expansion velocity in the transverse plane is studied in a transport model approach and is found to have transverse sphericity dependence indicating that the isotropic events can have more radial flow compared to the jetty events [12, 13].

These radial flow-like effects in pp collisions using PYTHIA8 are shown to have proportionality with the number of multi-partonic interactions (N_{mpi}). The high value of N_{mpi} is prone to have enhanced radial flow-like effects [14]; while the effects are reduced for low N_{mpi} . However, in experiments, it is impossible to measure N_{mpi} directly. Event shape-based studies are one such method to probe N_{mpi} as they show a significant correlation in simulations. Transverse sphericity being an event-shape observable, is capable of separating the

*Corresponding author: raghunath.sahoo@cern.ch

events based on geometrical shapes [15]. It can identify the soft-QCD-dominated isotropic events and the hard-QCD-dominated jetty events from the average events. This feature of transverse sphericity makes it a perfect tool for studying the QGP-like signatures in small collision systems [13, 15–22]. Another crucial point to note is that transverse sphericity is usually defined in the midrapidity ($|\eta| < 0.8$) due to the current detector charged-particle measurement constraints at the LHC in the forward pseudorapidities. However, keeping ALICE 3 upgrades at the LHC in mind, this study aims to demonstrate the sphericity and pseudorapidity dependence, where we define the transverse sphericity in a broader range of pseudorapidity. In this manuscript, we study the observables which are sensitive to radial-flow-like effects such as the mean transverse momentum, particle ratios, and kinetic freezeout parameters as a function of transverse sphericity and pseudo-rapidity in pp collisions at $\sqrt{s} = 13$ TeV using PYTHIA8.

The paper is organized as follows. We start with a brief introduction in Sec. I, then discuss the event generation using PYTHIA8 and transverse sphericity in Sec. II, then discuss the observables, and results in Sec. III. Finally, we summarise our findings in Sec. IV.

II. EVENT GENERATION AND METHODOLOGY

In this section, we discuss the event generation models, tunes, and analysis methodology. We start the description with the pQCD-inspired PYTHIA8 model and then discuss transverse sphericity.

A. PYTHIA8

PYTHIA is a widely used perturbative QCD-inspired MC event generator to simulate hadronic, leptonic, and heavy-ion collisions with emphasis on physics related to small collision systems like pp collisions [7]. PYTHIA8 involves soft and hard QCD processes and contains the libraries for initial and final state parton showers, multiple parton-parton interactions, beam remnants, string fragmentation, and particle decays. In our present study, we have implemented the default 4C tune of PYTHIA8 (version 8.308) with the multi-partonic interactions (MPI) and color reconnection (CR) mechanisms involving soft-QCD processes and hadronic decays [23, 24]. The particles originating from the MPIs and the beam remnants form the underlying event. The Lund-string fragmentation model performs the hadronisation of these partons [23]. The CR picture makes sure that the string between the partons is arranged in such a way that the total string length is reduced, which in turn leads to reduced particle multiplicity of the event. The 4C tune [24] based on MPI and CR is able to reproduce many features of the experimental pp collisions data reasonably well. Figure 13

shows the comparison of the above-mentioned tunes of PYTHIA8 with the ALICE measurements from Ref. [25] for transverse momentum spectra of minimum bias pp collisions at $\sqrt{s} = 13$ TeV. As shown, the PYTHIA8-based 4C tune overestimates the experimental data by a factor of 0.15; however, the trend of the experimental transverse momentum spectra is well reproduced by PYTHIA8 within 10% uncertainties.

B. Transverse Sphericity

Transverse sphericity is a well-established event shape classifier in pp collisions, capable of separating the p-QCD dominated events from the soft-QCD events. Due to its unique feature to identify and separate the rare pp collisions, transverse sphericity-based selections are useful for studying these QGP signatures. It is also observed that the selections based on the transverse sphericity, indeed, can identify the events with enhanced production of strange hadrons [26], similar to radial flow effects [19] in pp collision. The transverse sphericity, an infrared and co-linear safe quantity, is defined for a unit vector $\hat{n}(n_T, 0)$ in the transverse plane as [15],

$$S_0 = \frac{\pi^2}{4} \min_{\hat{n}} \left(\frac{\sum_{i=1}^{N_{\text{had}}} |\mathbf{p}_T \times \hat{n}|}{\sum_{i=1}^{N_{\text{had}}} |\mathbf{p}_T|} \right)^2 \quad (1)$$

In Eq.1, \hat{n} is chosen such that the ratio is minimized. The summations run over all the charged hadrons, and N_{had} is the total number of charged hadrons. Multiplication of $\pi^2/4$ in Eq.1 makes S_0 to lie between 0 and 1. The extreme limits of S_0 represent specific configurations of events in the transverse plane. The lower limit of transverse sphericity ($S_0 \rightarrow 0$) characterizes hard jetty events with back-to-back pencil-like structures, while the higher limit ($S_0 \rightarrow 1$) corresponds to soft isotropic events. In this study, transverse sphericity is determined using the charged hadrons in the pseudorapidity range, $|\eta| < 2.0$ having transverse momentum, $p_T > 0.15$ GeV/c. Categorization into the jetty and isotropic classes are done by choosing transverse sphericity cuts corresponding to the lowest 20% and highest 20% events in the sphericity distribution, respectively. For the sake of simplicity, we may sometimes refer to transverse sphericity as sphericity.

Figure 1 compares the minimum bias transverse sphericity distribution for pp collisions at $\sqrt{s} = 13$ TeV using PYTHIA8 for the sphericity defined for the particle tracks in the conventional pseudorapidity range $|\eta| < 0.8$ with the sphericity in the pseudorapidity range $|\eta| < 2.0$. Here, the peak of S_0 distribution is shown to be shifted to a higher sphericity limit as we broaden the rapidity region for transverse sphericity from $|\eta| < 0.8$ to $|\eta| < 2.0$. This is because the inclusion of a broader pseudorapidity bin leads to more charged particle tracks distributed over the ϕ -region, which in turn, according to Eq. 1, leads to higher values of S_0 . In addition, the inclusion of the

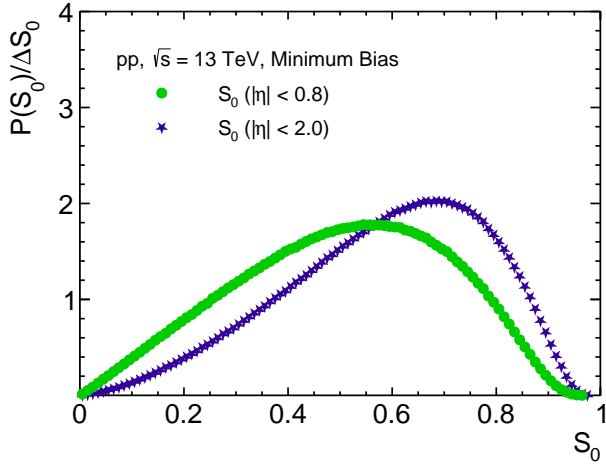


FIG. 1: (Color online) Transverse sphericity distribution ($S_0(|\eta| < 0.8)$ and $S_0(|\eta| < 2.0)$) in pp collisions at $\sqrt{s} = 13$ TeV using PYTHIA8.

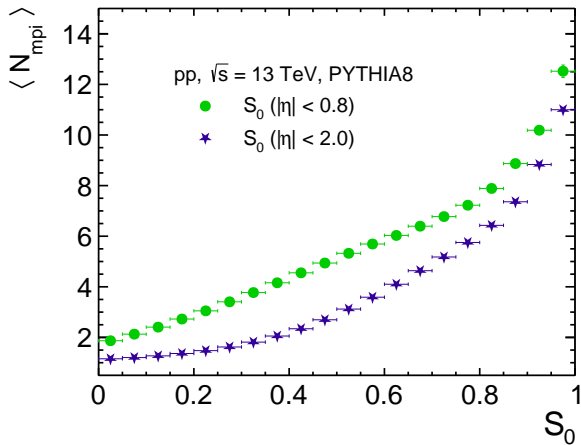


FIG. 2: (Color online) Mean number of multipartonic interactions ($\langle N_{mpi} \rangle$) as a function of transverse sphericity.

broader pseudorapidity bin for the definition of S_0 also affects its correlation with the N_{mpi} , as shown in Fig 2. Here, $\langle N_{mpi} \rangle$ is shown as a function of S_0 defined in two different pseudorapidity bins. Both the definitions of transverse sphericity are observed to possess a higher degree of correlation with N_{mpi} . It is found that the sphericity defined in a narrower bin achieves a higher $\langle N_{mpi} \rangle$ value for the most isotropic events as compared to the sphericity defined in the broader pseudorapidity region. In contrast, the sphericity in the wider region can probe towards a lower value of N_{mpi} . This is expected as the transverse sphericity is correlated with the number of charged particles irrespective of the defined pseudorapidity region. Thus, the inclusion of a wider pseudorapidity region makes a semi-soft event seem softer while the hard events are not much affected by it. This effect makes

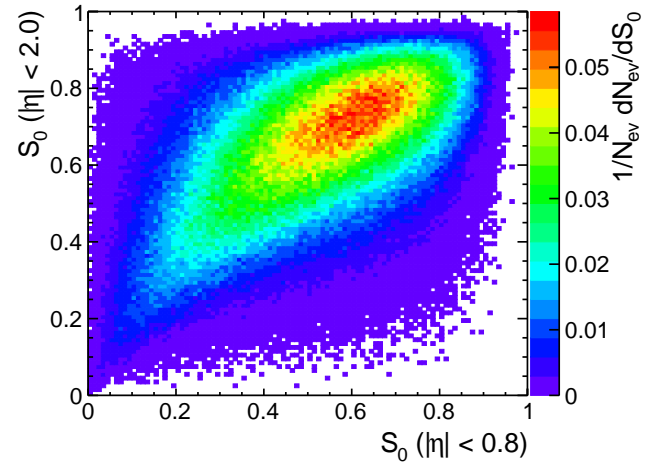


FIG. 3: (Color online) Correlation between S_0 measured in $|\eta| < 0.8$ and $|\eta| < 2.0$.

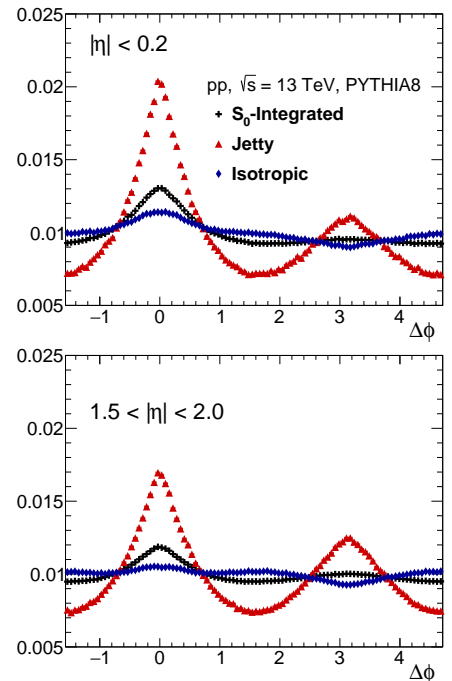


FIG. 4: (Color online) Sphericity dependence of $\Delta\phi$ distributions for charged-particles in $|\eta| < 0.2$ and $1.5 < |\eta| < 2.0$.

$S_0(|\eta| < 2.0)$ a little insensitive to the high N_{mpi} values while sensitive to low values of N_{mpi} . In other words, $S_0(|\eta| < 0.8)$ is a good probe to separate the isotropic events while $S_0(|\eta| < 2.0)$ can handle the hard events better. This can be verified via the correlation between $S_0(|\eta| < 2.0)$ and $S_0(|\eta| < 0.8)$ as shown in Fig. 3. Fig. 4 shows the sphericity dependence of $\Delta\phi$ distributions for charged-particles in $|\eta| < 0.2$ and $1.5 < |\eta| < 2.0$ ranges. As can be seen in the figures, the disentangling power of sphericity remains intact with the broader pseudorapidity range for sphericity calculation.

VOM Percentile	$\langle dN_{\text{ch}}/d\eta \rangle$	S_0 range	
		Jetty	Isotropic
0 - 1	25.323 ± 0.017	0 - 0.675	0.865 - 1
1 - 5	20.074 ± 0.007	0 - 0.645	0.845 - 1
5 - 10	16.427 ± 0.058	0 - 0.615	0.835 - 1
10 - 20	12.903 ± 0.004	0 - 0.585	0.815 - 1
20 - 30	9.550 ± 0.003	0 - 0.535	0.795 - 1
30 - 40	7.054 ± 0.003	0 - 0.485	0.765 - 1
40 - 50	5.091 ± 0.002	0 - 0.425	0.735 - 1
50 - 70	3.377 ± 0.001	0 - 0.355	0.695 - 1
0 - 100	6.702 ± 0.002	0 - 0.425	0.765 - 1

TABLE I: Transverse sphericity cuts for the jetty and isotropic events for different multiplicity classes in pp collisions at $\sqrt{s} = 13$ TeV using PYTHIA8.

In this study, the charge multiplicity selection is made in the V0 detector acceptance region (VOM) of the ALICE experiment at the LHC, *i.e.*, $-3.7 < \eta < -1.7$ and $2.8 < \eta < 5.1$ [27]. Corresponding percentile cuts for the VOM selection are listed in Tab. I along with the class name that would be used throughout the study. In addition, the table includes corresponding mean charge particle density measured in the mid-rapidity region, *i.e.*, $|\eta| < 2.0$ along with the sphericity cuts for jetty and isotropic events in each VOM class. Here, the differential study for pseudorapidity is performed in six pseudorapidity regions, *viz.*, $|\eta| < 0.2$, $0.2 \leq |\eta| < 0.4$, $0.4 \leq |\eta| < 0.7$, $0.7 \leq |\eta| < 1$, $1 \leq |\eta| < 1.5$ and $1.5 \leq |\eta| < 2$.

III. RESULTS AND DISCUSSIONS

In this section, we present the results on the observables such as particle ratios, mean transverse momentum, and kinetic freezeout properties, which are believed to be sensitive to the radial flow effects.

A. Particle ratios

As the radial flow is expected to give a larger boost to the particles with higher mass compared to the lower mass particles, the observed broadening in p_T spectra is expected to be different for particles with varying masses. In Ref. [9], authors have explicitly discussed the effect of radial flow for different particles. It has been observed that the p_T spectra of pions, in the presence of a strong radial flow, acquire a ‘convex’ shape while protons develop a positive curvature. The slopes of the p_T spectra of all particles become less steep in the presence of radial flow. This particle mass-dependent modification in the particle p_T spectra in the presence of radial flow reflects in the p_T -dependent yield ratios of different masses. In

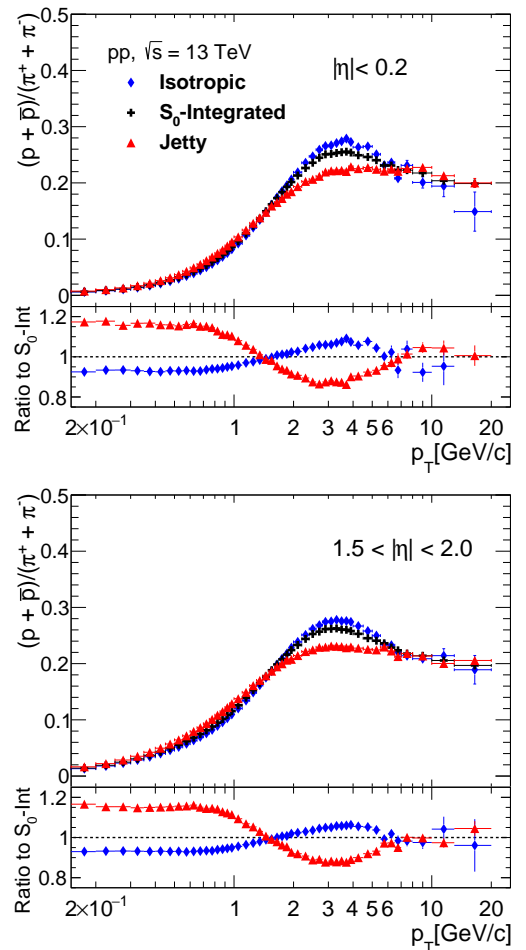


FIG. 5: (Color online) Proton-to-pion ratio as a function of transverse momentum for different sphericity bins in pp collisions at $\sqrt{s} = 13$ TeV for the pseudorapidity selection of $|\eta| < 0.2$ (top) and $1.5 < |\eta| < 2.0$ (bottom).

Pb–Pb collisions at $\sqrt{s_{\text{NN}}} = 2.76$ TeV, the proton-to-pion ratio measurement exhibits a strong enhancement in the intermediate p_T region compared to pp collisions of the same range [10]. This enhancement decreases as one moves from central to peripheral Pb–Pb collisions [10]. The amplitude of the peak observed in the proton-to-pion production ratio indicates the strength of the radial flow effect. But such radial flow-like signals are recently observed in high multiplicity proton-proton collisions [4, 5], which were otherwise taken as the baseline measurement for heavy-ion collisions. Here using PYTHIA8, we try to investigate the possible source and behaviour of this peak in the particle ratios of different masses in pp collisions at $\sqrt{s} = 13$ TeV. For simplicity, we denote $(p + \bar{p})/(\pi^+ + \pi^-)$ ratio as p/π ratio.

Figure 5 shows the proton-to-pion ratio as a function of p_T for $|\eta| < 0.2$ and $1.5 < |\eta| < 2.0$ ranges. For both the pseudorapidity ranges, isotropic events show a bigger bump structure in intermediate p_T with respect to the sphericity-integrated events. This is a testimony

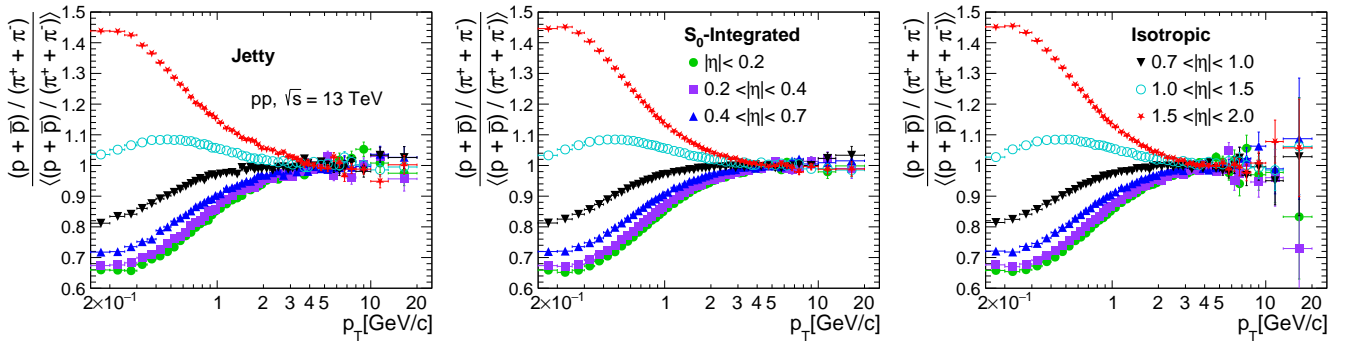


FIG. 6: (Color online) Proton-to-pion ratio normalized to their ratios in the full pseudorapidity range as a function of transverse momentum for different pseudorapidity bins in pp collisions at $\sqrt{s} = 13$ TeV for jetty (left), sphericity-integrated (middle) and isotropic (right) events.

that with sphericity selection, we are able to separate the rare events which show an enhanced-radial flow-like behavior. At the same time, the jetty events show a saturation behavior, indicating no radial flow-like effect. This peak-like structure is attributed to color reconnection in PYTHIA8 which is analogous to the peaks in the p/π ratio of Pb–Pb collisions due to radial flow effect. However, it is to be noted here that, the ratio does not show significant pseudorapidity dependence.

To investigate more on the pseudorapidity dependence, the p_T -dependent p/π ratio is normalized to the same in the entire pseudorapidity range, i.e. $|\eta| < 2.0$ which is shown in Fig. 6. The double p/π ratio as a function of p_T shows a significant dependence on pseudorapidity selection for $p_T < 2$ GeV/c for all sphericity classes. The double p/π ratio shows about 40% suppression (enhancement) for $|\eta| < 0.2$ ($1.5 < |\eta| < 2$) selection at the lowest p_T range. Then the double ratio approaches a similar value and beyond $p_T \simeq 2$ GeV/c, it seems to be independent of pseudorapidity selection. This is an important finding as this behavior shows that the radial flow-like feature, indicated by the bump-like structure in p/π ratio at $p_T \simeq 2 - 6$ GeV/c, is mildly affected by the pseudorapidity selection. However, the production of soft protons compared to soft pions is higher at forward-pseudorapidity when compared to the same with mid-pseudorapidity selection. It is also interesting to note that for a fixed pseudorapidity selection, the double ratios show a negligible sphericity dependence indicating, sphericity preserves the capability of finding the rare events with enhanced radial flow-like effects, irrespective of pseudorapidity selection.

B. Partonic modification factor (R_{pp})

Experimental measurements of identified particle production as a function of charged-particle multiplicity indicate a stronger than linear increase of high- p_T particle yields relative to minimum-bias pp collisions (the self-normalized yields) with the increase in midrapid-

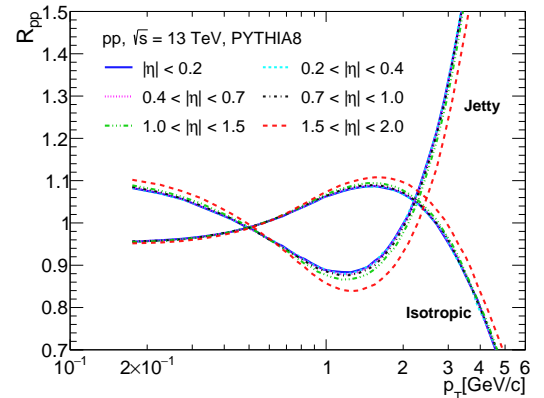


FIG. 7: (Color online) R_{pp} as a function of p_T for all charged hadrons for jetty and isotropic events within different pseudorapidity selections.

ity charged-particle multiplicity [28]. This effect is understood as a consequence of a bias due to event-selection [29]. To reduce such autocorrelation biases, the classification of events has been performed using forward pseudorapidity charged-particle multiplicity measurements in a different pseudorapidity interval to that where the observable of interest is measured [30]. Based on PYTHIA8 simulations the charged particle multiplicity measured in forward pseudorapidity is stronger correlated to the MPI activity [31]. However, the autocorrelation bias is still observed [32] which affects the observables that aim to search for medium-modification and partonic energy loss in small collision systems [33]. Thus, transverse sphericity, a key event shape classifier plays an important role in this direction to reduce the sensitivity to hard processes compared to classifiers based only on forward pseudorapidity charged-particle multiplicity estimation.

In heavy-ion collisions, traditionally one of the observables constructed to understand how particle production in heavy-ion collisions differs from the baseline proton-proton collisions is the nuclear modification factor, R_{AA} .

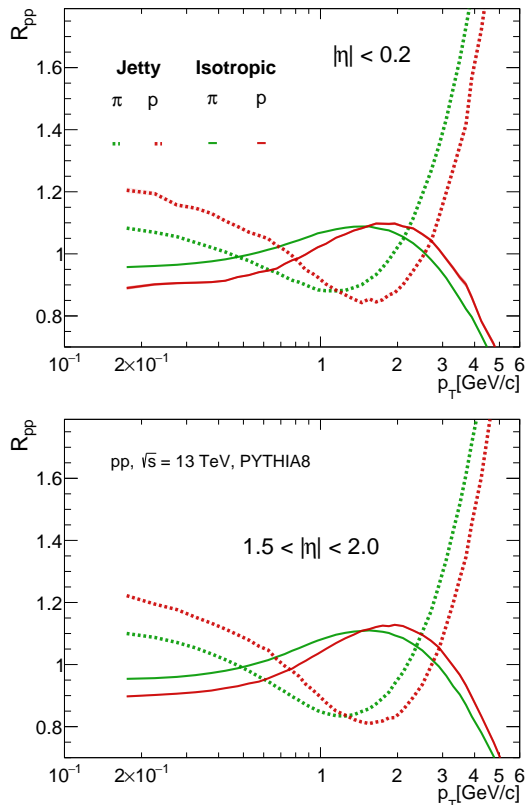


FIG. 8: (Color online) R_{pp} as a function of p_T for pions and protons for jetty and isotropic events in extreme η classes i.e. $|\eta| < 0.2$ (top) and $1.5 < |\eta| < 2.0$ (bottom).

It is defined as the ratio of yield in heavy-ion collisions (A–A) to that of the yield in pp collisions normalized by the average number of binary collisions [11, 34].

$$R_{AA} = \frac{1}{\langle N_{\text{coll}} \rangle} \frac{d^2 N_{AA}/d\eta dp_T}{d^2 N_{pp}/d\eta dp_T}, \quad (2)$$

where the numerator is the p_T spectra in heavy-ion collisions while the denominator is the scaled p_T spectra in pp collisions by the total number of average binary pp collisions in a single A–A collision. In the absence of QGP medium formation, the yield in a single A–A collision is expected to be simply a linear superposition of the yield in the pp collisions times the number of binary pp collisions in a single A–A collision. This gives rise to the condition of $R_{AA} = 1$, suggesting no medium effect. $R_{AA} < 1$ ($R_{AA} > 1$) for identified particles indicates a suppression (enhancement) of hadrons which can be attributed to the presence of QGP medium.

Since in our study, the system under focus is a proton-proton collision system and as the baseline used in the definition of nuclear modification factor is also a pp system, there is a requirement to redefine the modification factor accordingly. In Ref. [14], the authors have introduced a quantity motivated from R_{AA} , i.e., R_{pp} . We refer to this quantity as partonic modification factor. This is

defined as the normalized ratio of the yield of all charged particles in a specific sphericity class and a particular pseudorapidity bin to their yield in the same pseudorapidity bin for S_0 -integrated events.

$$R_{pp} = \frac{d^2 N_{\text{ch}}^{S_0} / \langle N_{\text{ch}}^{S_0} \rangle d\eta dp_T}{d^2 N_{\text{ch}}^{\text{MB}} / \langle N_{\text{ch}}^{\text{MB}} \rangle d\eta dp_T} \Big|_{\eta} \quad (3)$$

Analogous to the $1/\langle N_{\text{coll}} \rangle$ in R_{AA} , here we normalise the yields with respect to the average charged particle multiplicity in the corresponding sphericity event class i.e. the normalization constant used for scaling here is $\langle N_{\text{ch}}^{\text{MB}} \rangle / \langle N_{\text{ch}}^{S_0} \rangle$.

As can be seen in Fig. 7, R_{pp} for jetty events has initially, a decreasing trend in the intermediate p_T region after which it rapidly rises towards higher p_T domains. On the other hand, R_{pp} for isotropic events increases first and then drops, showing a suppression trend. This behavior is very similar when one studies R_{pp} as a function of number of multiparton interactions as shown in Ref. [14]. These enhancement and suppression trends in the yields for jetty and isotropic events have a mild dependence on pseudorapidity, however, for the forward pseudorapidity range, the enhancement and suppression are steeper.

Figure 8 shows R_{pp} as a function of p_T for pions and protons for jetty and isotropic events in extreme η classes i.e. $|\eta| < 0.2$ and $1.5 < |\eta| < 2.0$. A similar behavior is observed for both pions and protons as seen in Fig. 7. However, the key point to note from Fig. 8 is that a significant mass-dependent shift of peak position of enhancement and suppression at intermediate- p_T is observed for jetty and isotropic events, respectively. This feature is attributed to the color reconnection mechanism in PYTHIA8 and is seen as radial-flow-like effect. This behavior has a negligible dependence on the pseudorapidity selection.

C. Mean transverse momentum

Radial flow is understood as the collective expansion of the hot dense medium formed in relativistic collisions in a direction radially outward. The matter formed in such high-energy collisions expands and cools, and it undergoes a phase transition from the deconfined partonic state to that of a hadronic state. These produced hadrons are also carried along with the flow. As this system reaches the kinetic freeze-out, the momentum distributions of produced hadrons become fixed. In the absence of radial flow, the p_T spectra of particles in the low p_T region are expected to follow a thermal Boltzmann distribution. However, in the presence of radial flow, these exponential shapes are found to get modified [9]. This happens due to the fact that radial flow induces a boost to the produced particles, which is reflected in their transverse momentum spectra. The effect is such that the high transverse momentum particles acquire a more significant

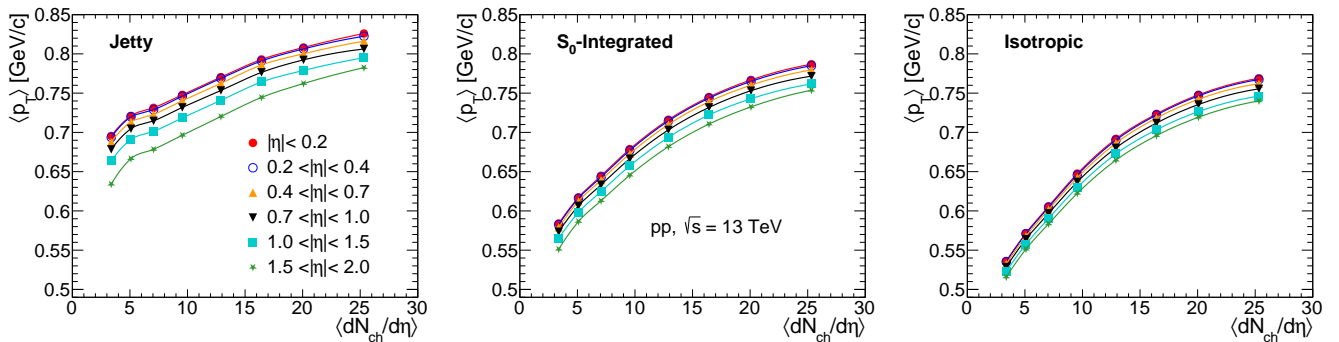


FIG. 9: (Color online) $\langle p_T \rangle$ versus $\langle dN_{ch}/d\eta \rangle$ as a function of pseudorapidity for jetty, S_0 -integrated and isotropic events in pp collisions at $\sqrt{s} = 13$ TeV using PYTHIA8.

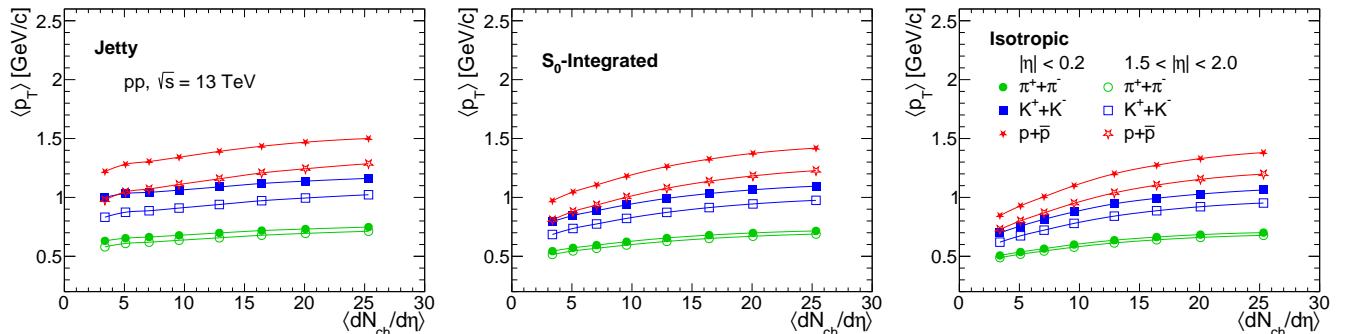


FIG. 10: (Color online) $\langle p_T \rangle$ versus $\langle dN_{ch}/d\eta \rangle$ for pions, kaons and protons as a function of extreme pseudorapidity classes for jetty, S_0 -integrated and isotropic events in pp collisions at $\sqrt{s} = 13$ TeV using PYTHIA8.

boost compared to those with low transverse momentum. This leads to p_T broadening and shifting of the entire p_T spectra to higher values of transverse momenta, thus increasing the mean transverse momentum ($\langle p_T \rangle$) of the produced hadrons.

Figure 9 shows $\langle p_T \rangle$ as a function of charged particle density for the jetty (left), S_0 -integrated (middle) and isotropic (right) events estimated in different regions of pseudorapidity in pp collisions at $\sqrt{s} = 13$ TeV. The $\langle p_T \rangle$ is calculated in the region $0.15 < p_T < 10$ GeV/c. For all pseudorapidity selections, the $\langle p_T \rangle$ increases with $\langle dN_{ch}/d\eta \rangle$. This enhancement of $\langle p_T \rangle$ with multiplicity follows a similar trend as observed in Pb-Pb collisions and can be attributed to the higher radial flow-like effects with an increase in the charged particle density due to the presence of higher N_{mpi} [35]. Here, one observes significant pseudorapidity dependence of $\langle p_T \rangle$. The value of $\langle p_T \rangle$ decreases with increased pseudorapidity. Since the mid-pseudorapidity regions, where the gluons dominate the particle production, are denser compared to forward pseudorapidities where the particle production is dominated by fragmentation and hadronic decays. The particle production is less favoured at higher pseudorapidities compared to the midrapidities. Thus, the radial flow is more probable in mid- η regions due to large particle density in the mid-pseudorapidity. In addition, the expansion of the created matter in the longitudinal direc-

tion (forward- η) is faster than in the mid-pseudorapidity region. A faster longitudinal expansion would reduce the time for the radial flow to develop, resulting in less radial flow effects observed in forward-pseudorapidity [11]. On the other hand, $\langle p_T \rangle$ is found to show sphericity dependence, where $\langle p_T \rangle$ is higher for jetty events compared to the isotropic events throughout the pseudorapidity bins. The observed higher value of $\langle p_T \rangle$ for the jetty events are because of contribution due to the domination of jets.

To understand the pseudorapidity dependence of $\langle p_T \rangle$ in greater detail, in Fig. 10, $\langle p_T \rangle$ as a function of charged particle density for pions ($\pi^+ + \pi^-$), kaons ($K^+ + K^-$) and protons ($p + \bar{p}$) is studied for the jetty, S_0 -integrated and isotropic events in the extreme pseudorapidity selections in pp collisions at $\sqrt{s} = 13$ TeV. As the radial flow gives a larger boost to heavier particles, a clear mass ordering is observed where $\langle p_T \rangle$ is more for protons than kaons and the least for pions. As expected from the trends observed in Fig. 9, mid-pseudorapidity hadrons show a significant enhancement $\langle p_T \rangle$ than that of forward-pseudorapidity hadrons. This drop of $\langle p_T \rangle$ from mid to forward pseudorapidity, with a more pronounced effect on heavier hadrons, once again reflects the diminishing effect of radial flow towards higher pseudorapidities [11].

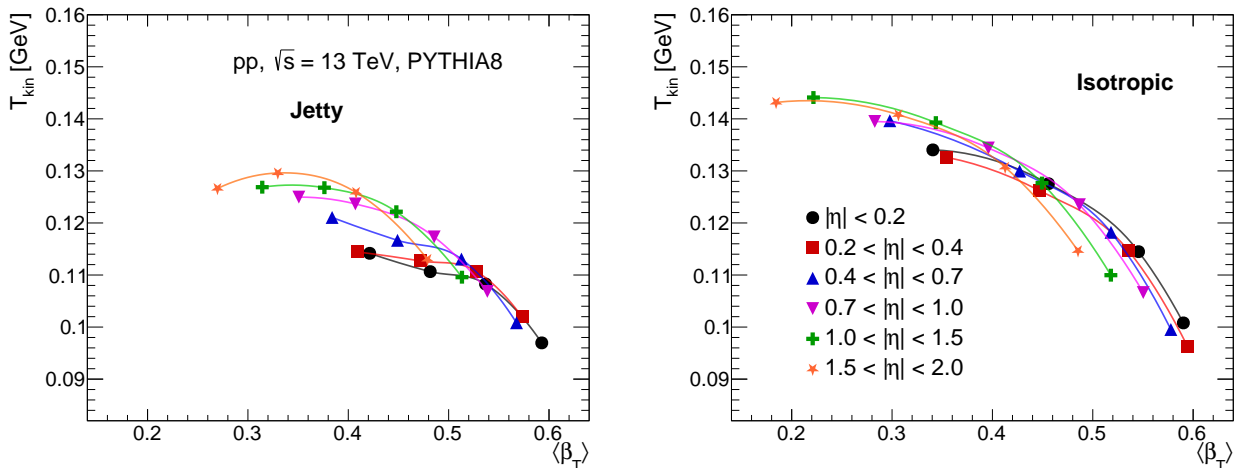


FIG. 11: (Color online) Kinetic freeze-out temperature versus mean transverse radial flow velocity as a function of pseudorapidity for jetty (left) and isotropic (right) events from the simultaneous blastwave fitting of the p_T spectra of protons, kaons, and pions.

D. Kinetic freezeout parameters

The space-time evolution in ultra-relativistic collisions involves several phases. The traditional heavy-ion picture assumes the pre-equilibrium phase, the QGP phase, the mixed phase, the chemical freeze-out, the hadron gas phase, and finally, the kinetic freeze-out phase. The effect of radial flow thus migrates from the partonic QGP phase to the hadron gas phase and survives till the kinetic freeze-out giving a boost to the produced hadrons. This results in the enhancement of the expansion velocity of the hadronic system. This expansion velocity is imprinted in the transverse momentum spectra of the produced hadrons. One can extract the expansion velocity along with the kinetic freeze-out temperature by a simultaneous fitting of the Boltzmann-Gibbs blastwave (BGBW) function to the identified particles' transverse momentum spectra measured after the kinetic freeze-out. The BGBW function at midrapidity is given by the following expression [11, 36]:

$$\left. \frac{d^2N}{dp_T dy} \right|_{y=0} = C p_T m_T \int_0^{R_0} r n(r) dr K_1 \left(\frac{m_T \cosh \rho}{T_{\text{kin}}} \right) I_0 \left(\frac{p_T \sinh \rho}{T_{\text{kin}}} \right) \quad (4)$$

where $K_1 \left(\frac{m_T \cosh \rho}{T_{\text{kin}}} \right)$ and $I_0 \left(\frac{p_T \sinh \rho}{T_{\text{kin}}} \right)$ are modified Bessel's functions, which are given by,

$$K_1 \left(\frac{m_T \cosh \rho}{T_{\text{kin}}} \right) = \int_0^\infty \cosh y \exp \left(- \frac{m_T \cosh y \cosh \rho}{T_{\text{kin}}} \right) dy, \quad (5)$$

$$I_0 \left(\frac{p_T \sinh \rho}{T_{\text{kin}}} \right) = \frac{1}{2\pi} \int_0^{2\pi} \exp \left(\frac{p_T \sinh \rho \cos \phi}{T_{\text{kin}}} \right) d\phi, \quad (6)$$

where, $\rho = \tanh^{-1} \beta_T$ and $\beta_T = \beta_s \xi^n$ [36–39]. β_T is called radial flow, β_s is the maximum surface velocity, $\xi = (r/R_0)$ with r being the radial distance and R_0 the maximum radius of the source at freeze-out. $n(r)$ is the nuclear density profile; in our study, we have considered $n(r) = 1$ for $r < R_0$ and $n(r) = 0$ for $r > R_0$, i.e., hard sphere profile. In this model, the particles closer to the center of the fireball are assumed to move slower than the ones at the edges. The mean transverse velocity is given by [40],

$$\langle \beta_T \rangle = \frac{\int \beta_s \xi^n \xi d\xi}{\int \xi d\xi} = \left(\frac{2}{2+n} \right) \beta_s. \quad (7)$$

In Eq. 4, the modified Bessel's function comes as a consequence of the integration from $-\infty$ to $+\infty$ over pseudorapidity η , assuming boost invariance. However, as one goes towards the forward rapidity, the condition of boost invariance is not valid. Thus, the modified Bessel's function should be replaced by an integral, i.e., $g(z)$ for $z = m_T \cosh \rho / T_{\text{kin}}$ over a finite range of η , defined as follows [11].

$$g(z) = \int_{\eta_{\text{min}}}^{\eta_{\text{max}}} \cosh(\eta - y) e^{-z \cosh(\eta - y)} d\eta \quad (8)$$

Now, the substitution of Eq. 8 in Eq. 4 modifies as follows:

$$\left. \frac{d^2N}{dp_T dy} \right|_{y=0} = C p_T m_T \int_0^{R_0} r n(r) dr g \left(\frac{m_T \cosh \rho}{T_{\text{kin}}} \right) I_0 \left(\frac{p_T \sinh \rho}{T_{\text{kin}}} \right) \quad (9)$$

Using Eq. 9, one can perform the simultaneous fitting to the transverse momentum spectra of pions ($\pi^+ + \pi^-$),

kaons ($K^+ + K^-$) and protons ($p + \bar{p}$). In Eq. 8, the value of y is chosen to be a pseudorapidity which lies exactly in the center of the polar angles corresponding to η_{\min} and η_{\max} . We use the similar fitting range from Ref. [19], i.e., $0.5 < p_T < 1$ GeV/c for pions, $0.3 < p_T < 1.5$ GeV/c for kaons and $0.8 < p_T < 2.0$ GeV/c for protons. The values obtained from fitting for $\langle\beta_T\rangle$ and T_{kin} as well as the corresponding χ^2/NDF values are tabulated in Table II. Kinetic freeze-out temperature (T_{kin}) versus mean transverse radial flow velocity ($\langle\beta_T\rangle$) as a function of transverse sphericity for two extreme pseudorapidity selections are plotted in Fig. 11. T_{kin} and $\langle\beta_T\rangle$ are found to be multiplicity dependent. Higher multiplicity classes show increased flow velocity and decreased kinetic freeze-out temperature which ought to be due to the longer time it would require to reach the freeze-out [12]. A mild sphericity dependence is observed for both radial expansion velocity and kinetic freeze-out temperature.

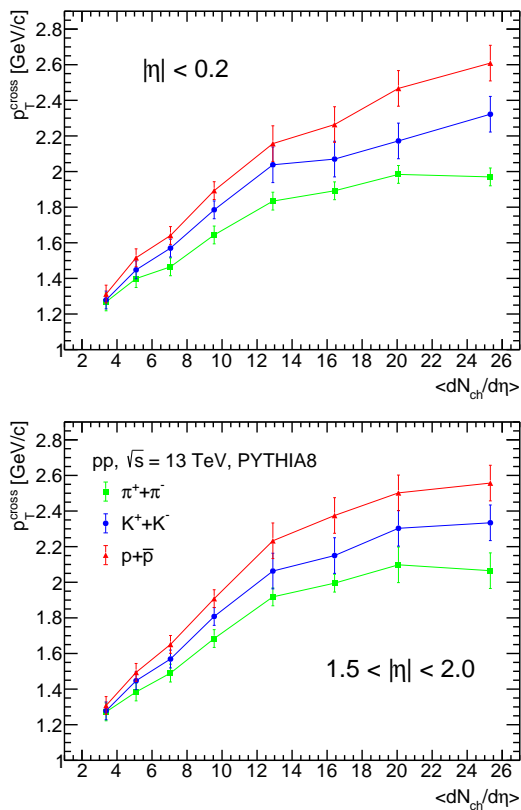


FIG. 12: (Color online) The crossing of the ratio of p_T spectra for isotropic and jetty events (p_T^{cross}) as a function of mean charged particle multiplicity density ($\langle dN_{\text{ch}}/d\eta \rangle$) for pions, kaons and protons in extreme pseudorapidity bins

E. Transverse momentum crossing points

The p_T values where the p_T spectra for jetty events start to dominate over the isotropic events are referred to as the p_T crossing points (p_T^{cross}). These crossing points

suggest that the production of hadrons is dominated by isotropic events in the low p_T and jetty events in the high p_T region [16]. Figure 12 shows p_T^{cross} for two extreme pseudorapidity selections studied as a function of mean charged particle multiplicity density ($\langle dN_{\text{ch}}/d\eta \rangle$) for pions, kaons and protons. As one can observe, the crossing of p_T spectra of isotropic and jetty events has a clear multiplicity dependence, and the crossing point shifts towards higher p_T with increasing multiplicity. This would imply that the soft particle production in high multiplicity collisions lasts to higher values in p_T compared to low multiplicity events.

Here, we also see a mass dependence where shifting of p_T crossing points to higher p_T is more for protons than kaons followed by pions and this could be attributed to a flow-like behaviour. This mass ordering is observed in all pseudorapidity windows with the mass dependence becoming clearer only for high multiplicity classes.

IV. SUMMARY

This study aims at exploring the pseudorapidity and transverse sphericity dependence of radial flow-like effects in pp collisions at $\sqrt{s} = 13$ TeV using the p-QCD inspired model PYTHIA8. Unlike the earlier definitions of sphericity in the pseudorapidity range $|\eta| < 0.8$, here, we redefine sphericity in the $|\eta| < 2.0$ region. With this modification in sphericity, we perform the differential studies of various observables that are known to be sensitive to the radial flow-like effects as a function of transverse sphericity, pseudorapidity (upto $|\eta| < 2.0$) and charged-particle multiplicity wherever possible. These observables include $\langle p_T \rangle$, particle ratios such as p/π , kinetic freezeout parameters such as T_{kin} and $\langle\beta_T\rangle$, partonic modification factor (R_{pp}) and the transverse momentum crossing points between the jetty and isotropic events. The findings are summarised below.

1. The mean number of multipartonic interactions has a direct correlation with the transverse sphericity.
2. The p/π ratio as a function of p_T shows a peak-like structure at around 3 GeV/c where the sphericity dependence also becomes clearly distinct. Peak exhibited by isotropic events are more prominent than jetty events due to more nMPIs, which shows that the flow-like effects are enhanced in isotropic events.
3. At low p_T , the p/π ratios are slightly higher for forward-pseudorapidity hadrons as compared to mid- η hadrons. Both the ratios saturate at higher p_T .
4. The isotropic events show lower $\langle p_T \rangle$ than the jetty events while $\langle p_T \rangle$ increases with an increase in the charged particle multiplicity and towards the central pseudorapidity regions, indicating effect from

η class	VOM Percentile	Isotropic			Jetty		
		$\langle\beta_T\rangle$	T [GeV/c]	χ^2/NDF	$\langle\beta_T\rangle$	T [GeV/c]	χ^2/NDF
$ \eta < 0.2$	0-1	0.590 ± 0.010	0.101 ± 0.007	0.547	0.593 ± 0.008	0.097 ± 0.005	0.833
	10-20	0.546 ± 0.013	0.114 ± 0.006	0.674	0.537 ± 0.009	0.108 ± 0.004	1.049
	30-40	0.456 ± 0.024	0.128 ± 0.008	1.260	0.482 ± 0.014	0.111 ± 0.006	0.833
	50-70	0.341 ± 0.042	0.134 ± 0.009	1.640	0.421 ± 0.018	0.114 ± 0.006	1.196
$0.2 < \eta < 0.4$	0-1	0.595 ± 0.010	0.096 ± 0.007	0.528	0.573 ± 0.012	0.102 ± 0.009	0.539
	10-20	0.535 ± 0.013	0.115 ± 0.006	0.674	0.528 ± 0.010	0.111 ± 0.006	1.127
	30-40	0.447 ± 0.024	0.126 ± 0.008	0.909	0.472 ± 0.012	0.113 ± 0.005	1.321
	50-70	0.355 ± 0.038	0.133 ± 0.009	1.678	0.409 ± 0.017	0.114 ± 0.006	2.059
$0.4 < \eta < 0.7$	0-1	0.578 ± 0.013	0.100 ± 0.008	0.307	0.568 ± 0.012	0.101 ± 0.008	0.475
	10-20	0.518 ± 0.014	0.118 ± 0.007	0.525	0.513 ± 0.014	0.113 ± 0.007	0.546
	30-40	0.427 ± 0.027	0.130 ± 0.009	1.082	0.449 ± 0.017	0.117 ± 0.007	0.848
	50-70	0.298 ± 0.040	0.140 ± 0.008	1.463	0.384 ± 0.019	0.121 ± 0.006	0.880
$0.7 < \eta < 1.0$	0-1	0.550 ± 0.015	0.107 ± 0.009	0.275	0.539 ± 0.014	0.107 ± 0.008	0.664
	10-20	0.487 ± 0.015	0.124 ± 0.006	0.568	0.486 ± 0.015	0.117 ± 0.007	0.459
	30-40	0.396 ± 0.028	0.134 ± 0.008	0.851	0.407 ± 0.018	0.124 ± 0.006	0.631
	50-70	0.283 ± 0.037	0.140 ± 0.007	0.731	0.351 ± 0.023	0.125 ± 0.007	0.559
$1.0 < \eta < 1.5$	0-1	0.222 ± 0.021	0.144 ± 0.004	1.936	0.314 ± 0.017	0.127 ± 0.005	0.733
	10-20	0.344 ± 0.019	0.139 ± 0.005	1.236	0.376 ± 0.014	0.127 ± 0.005	0.900
	30-40	0.449 ± 0.012	0.128 ± 0.005	0.782	0.448 ± 0.012	0.122 ± 0.005	0.696
	50-70	0.518 ± 0.009	0.110 ± 0.005	0.527	0.513 ± 0.008	0.110 ± 0.004	0.542
$1.5 < \eta < 2.0$	0-1	0.485 ± 0.010	0.115 ± 0.005	0.515	0.479 ± 0.010	0.113 ± 0.005	0.616
	10-20	0.413 ± 0.013	0.131 ± 0.005	0.811	0.408 ± 0.012	0.126 ± 0.005	0.745
	30-40	0.306 ± 0.017	0.141 ± 0.004	1.322	0.330 ± 0.014	0.130 ± 0.004	0.856
	50-70	0.184 ± 0.026	0.143 ± 0.004	1.941	0.270 ± 0.014	0.127 ± 0.003	1.327

TABLE II: Kinetic freeze-out temperature (T_{kin}), mean transverse radial flow velocity ($\langle\beta_T\rangle$) and χ^2/NDF values obtained from a simultaneous fit of identified charged particles' p_T spectra with Boltzmann-Gibbs blastwave function as a function of multiplicity, pseudorapidity and transverse sphericity classes.

the larger radial flow. The mass dependence of $\langle p_T \rangle$ for different rapidity regions indicates that the heavier mass particles receive a higher boost compared to the lighter particles.

- The kinetic freeze-out parameters viz. T_{kin} and $\langle\beta_T\rangle$ have clear multiplicity dependence, where, an increase in multiplicity is associated with an enhanced flow velocity and a decreased kinetic freeze-out temperature.
- Isotropic and jetty events show suppression and enhancement trends in their normalized yield at higher p_T values, respectively. These effects are enhanced at the central pseudorapidity region.
- The transverse momentum crossing points have strong multiplicity dependence with p_T^{cross} shifting to higher values of p_T with increasing multiplicity. This indicates that the soft particle production lasts to higher values of p_T in high multiplicity events.
- The dependence of p_T^{cross} on $\langle dN_{\text{ch}}/d\eta \rangle$ also shows a mass-ordering at all pseudorapidity bins and this becomes clearer at higher multiplicities. The observed shift in p_T^{cross} with multiplicity is more for protons, followed by kaons and then pions, which might also be pointing at the flow-like behaviour.

V. ACKNOWLEDGEMENT

A.M.K.R. acknowledges the doctoral fellowships from the DST INSPIRE program of the Government of India. S.P. acknowledges the University Grants Commission (UGC), Government of India. The authors gratefully acknowledge the DAE-DST, Government of India funding under the mega-science project ‘‘Indian participation in the ALICE experiment at CERN’’ bearing Project No. SR/MF/PS-02/2021-IITI(E-37123).

Appendix

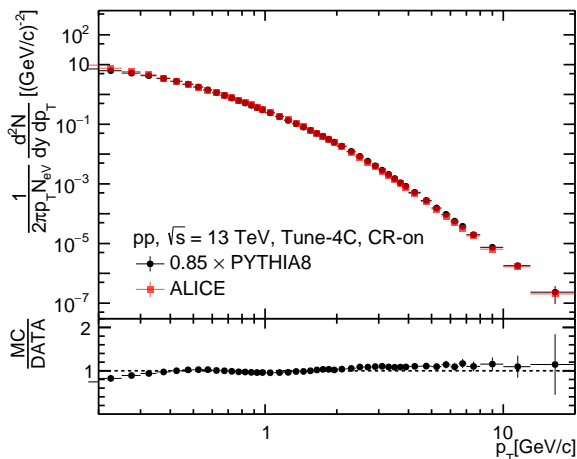


FIG. 13: (Color online) Comparison of PYTHIA8 generated data with ALICE results [25] for transverse momentum spectra of all charged hadrons for minimum bias pp collisions at $\sqrt{s} = 13$ TeV.

-
- [1] V. Khachatryan *et al.* [CMS], Phys. Rev. Lett. **116**, 172302 (2016).
- [2] B. B. Abelev *et al.* [ALICE], Phys. Lett. B **726**, 164 (2013).
- [3] J. Adam *et al.* [ALICE], Nature Phys. **13**, 535 (2017).
- [4] B. B. Abelev *et al.* [ALICE], Phys. Lett. B **728**, 25 (2014).
- [5] J. Adam *et al.* [ALICE], Phys. Lett. B **760**, 720 (2016).
- [6] V. Khachatryan *et al.* [CMS], Phys. Lett. B **765**, 193(2017).
- [7] T. Sjostrand, S. Mrenna and P. Z. Skands, Comput. Phys. Commun. **178**, 852 (2008).
- [8] A. Ortiz, G. Bencedi and H. Bello, J. Phys. G **44**, 065001 (2017).
- [9] A. Kisiel, Phys. Rev. C **84**, 044913 (2011).
- [10] R. Preghenella [ALICE], J. Phys. Conf. Ser. **455**, 012009 (2013).
- [11] I. C. Arsene *et al.* [BRAHMS], Phys. Rev. C **94**, 014907 (2016).
- [12] S. Prasad, N. Mallick, D. Behera, R. Sahoo and S. Tripathy, Sci. Rep. **12**, 3917 (2022).
- [13] S. Tripathy, A. Bisht, R. Sahoo, A. Khuntia and M. P. Salvan, Adv. High Energy Phys. **2021**, 8822524 (2021).
- [14] A. Ortiz, A. Paz, J. D. Romo, S. Tripathy, E. A. Zepeda and I. Bautista, Phys. Rev. D **102**, 076014 (2020).
- [15] E. Cuautle, R. Jimenez, I. Maldonado, A. Ortiz, G. Paic and E. Perez, arXiv:1404.2372 [hep-ph].
- [16] A. Khuntia, S. Tripathy, A. Bisht and R. Sahoo, J. Phys. G **48**, 035102 (2021).
- [17] S. Deb, S. Tripathy, G. Sarwar, R. Sahoo and J. e. Alam, Eur. Phys. J. A **56**, 252 (2020).
- [18] A. Khatun, D. Thakur, S. Deb and R. Sahoo, J. Phys. G **47**, 055110 (2020).
- [19] A. Ortiz, G. Paic and E. Cuautle, Nucl. Phys. A **941**, 78 (2015).
- [20] G. P. Salam, Eur. Phys. J. C **67**, 637 (2010).
- [21] G. Bencedi [ALICE], Nucl. Phys. A **982**, 507 (2019)
- [22] A. Banfi, G. P. Salam and G. Zanderighi, JHEP **1006**, 038 (2010).
- [23] B. Andersson, G. Gustafson, G. Ingelman and T. Sjostrand, Phys. Rept. **97**, 31 (1983).
- [24] R. Corke and T. Sjostrand, JHEP **03**, 032 (2011).
- [25] J. Adam *et al.* [ALICE], Phys. Lett. B **753**, 319 (2016).
- [26] A. Nassirpour, EPJ Web Conf. **259**, 13005 (2022).
- [27] B. B. Abelev *et al.* [ALICE], Int. J. Mod. Phys. A **29**, 1430044 (2014).
- [28] S. Acharya *et al.* [ALICE], Eur. Phys. J. C **79**, 857 (2019).
- [29] S. G. Weber, A. Dubla, A. Andronic and A. Morsch, Eur. Phys. J. C **79**, 36 (2019).
- [30] S. Acharya *et al.* [ALICE], Phys. Rev. C **99**, 024906 (2019).
- [31] A. Ortiz, A. Khuntia, O. Vázquez-Rueda, S. Tripathy, G. Bencedi, S. Prasad and F. Fan, Phys. Rev. D **107**, 076012 (2023).
- [32] S. Acharya *et al.* [ALICE], Eur. Phys. J. C **80**, no.8, 693 (2020).
- [33] S. Acharya *et al.* [ALICE], Phys. Lett. B **843**, 137649 (2023).
- [34] S. Acharya *et al.* [ALICE], Phys. Rev. C **101**, 044907 (2020).
- [35] B. B. Abelev *et al.* [ALICE], Phys. Lett. B **727**, 371(2013).
- [36] E. Schnedermann, J. Sollfrank and U. W. Heinz, Phys.

- Rev. C **48**, 2462 (1993).
- [37] P. Huovinen, P. F. Kolb, U. W. Heinz, P. V. Ruuskanen and S. A. Voloshin, Phys. Lett. B **503**, 58 (2001).
- [38] P. Braun-Munzinger, J. Stachel, J. P. Wessels and N. Xu, Phys. Lett. B **344**, 43 (1995).
- [39] Z. Tang *et al.*, Chin. Phys. Lett. **30**, 031201 (2013).
- [40] K. Adcox *et al.* [PHENIX], Phys. Rev. C **69**, 024904 (2004).